

Microstructures and Electrical Properties of RuO₂ Bottom Electrode for Ferroelectric Thin Films

Woong-Chul Shin, Cheol-Hoon Yang, Jun-Sik Hwang and Soon-Gil Yoon

Dept. of Materials Engineering, Chungnam National University, Daeduk Science Town, Taejeon, 305-764, Korea
(Received October 5, 1997)

RuO₂ thin films were deposited on Si(100) substrate at low temperatures by hot-wall metalorganic chemical vapor deposition. Bis(cyclopentadienyl)ruthenium, Ru(C₅H₅)₂, was used as the precursor. RuO₂ single phase was obtained at a low deposition temperature of 250°C and the crystallinity of RuO₂ thin films improved with increasing deposition temperature. RuO₂ thin films grow perpendicularly to the substrate and show the columnar structure. The grain size of RuO₂ films drastically increases with increasing the deposition temperature. The resistivity of the 180 nm-thick RuO₂ thin films deposited at 270°C was 136 μΩ-cm and increased with decreasing film thickness. SrBi₂Ta₂O₉ thin films deposited by rf magnetron sputtering on the RuO₂ bottom electrodes showed a fatigue-free characteristics up to ~10¹⁰ cycles under 5 V bipolar square pulses and the remanent polarization, 2 P_r, and the coercive field, 2 E_c, were 5.2 μC/cm² and 76.0 kV/cm, respectively, for an applied voltage of 5 V. The leakage current density was about 7.0 × 10⁻⁶ A/cm² at 150 kV/cm.

Key words : RuO₂, Metalorganic chemical vapor deposition, Resistivity, SrBi₂Ta₂O₉

I. Introduction

In recent years, ferroelectric thin films such as Pb(Zr, Ti)O₃(PZT) have been widely investigated for their applications in nonvolatile random access memory (NVRAM).¹⁻³ Although NVRAM devices conventionally used platinum as a bottom electrode, platinum electrode presents difficulties in the etching required to form the integrated structures.

Ruthenium dioxide with rutile structure exhibits metallic conductivity, excellent diffusion barrier properties, and high chemical corrosion resistance.^{4,5} RuO₂, as an electrode for ferroelectric thin film capacitors, has been investigated recently by several research groups since the use of RuO₂ as an electrode instead of Pt can avoid polarization fatigue of the capacitors.^{6,7}

So far, thin films of RuO₂ have mainly been prepared by rf magnetron sputtering,⁸ whereas work on metalorganic chemical vapor deposition (MOCVD) has been published rarely.^{1,9} A problem associated with the sputtered films is high film stress. It was found that the intrinsic stress of each of the sputtered films was compressive on the order of GPa. On the other hand, MOCVD is a valuable alternative method since it offers low cost, easy composition control, high deposition rate, excellent step coverage, and compatibility to large-scale processing. Green *et al.* have reported the preparation of MOCVD of RuO₂ and Ru thin films.⁴ In their studies, efforts had been made to select suitable precursors for MOCVD-RuO₂ thin films. For example, Ru(C₅H₅)₂, Ru₃(CO)₁₂ and Ru(C₅H₇O₂)₃ were used for RuO₂ deposition. Films deposited from

Ru₃(CO)₁₂ consisted entirely of Ru, regardless of the O₂, N₂, or vacuum ambient. Inferior quality RuO₂ films obtained from Ru(C₅H₇O₂)₃ consisted of large columnar grains which resulted in a very high electrical resistivity of 643 μΩ-cm. Only Ru(C₅H₅)₂ was found to be promising. In this study, Bis(cyclopentadienyl)ruthenium, Ru(C₅H₅)₂, was used as the precursor.

The resistivity of the RuO₂ thin films was affected by the deposition temperature, the oxygen partial pressure, the thickness of the film and the annealing conditions.^{10,11}

In this study, RuO₂ thin films were prepared on Si(100) by hot-wall MOCVD and the ferroelectric SrBi₂Ta₂O₉ thin films were deposited on the MOCVD-RuO₂ films by rf magnetron sputtering. The microstructure and the electrical properties of the RuO₂ thin films were evaluated and the ferroelectric properties of SrBi₂Ta₂O₉ thin films deposited on MOCVD-RuO₂ were also investigated.

II. Experimental

Hot-wall MOCVD system was used for RuO₂ thin film growth at low temperature. Ru(C₅H₅)₂ as precursor and oxygen as reaction gas were used to grow the RuO₂ thin films and RuO₂ thin films were deposited onto Si(100) wafer of 3 × 3 (cm²) size. The deposition conditions of RuO₂ thin films were tabulated in Table 1.

Bi-layered SrBi₂Ta₂O₉ (SBT) thin films were deposited on RuO₂/Si using rf magnetron sputtering. The composition of the target was a Sr_{1.2}Bi_{2.1}Ta_{2.0}O₉ ceramic to compensate for the deficiency of Sr and Bi in SBT films, and Bi target was used simultaneously with the SBT tar-

Table 1. Deposition Conditions for RuO₂ Thin Films Preparation

Source material	Ru(C ₅ H ₅) ₂
Bubbling temperature	75°C
Carrier gas (Ar) flow rate	100 sccm
Reaction gas (O ₂) flow rate	200 sccm
Deposition temperature	220~300°C
Deposition time	1 h
Deposition pressure	3 torr
Substrate	Si(100)

Table 2. Sputtering Conditions for SBT Thin Films Preparation

Target materials	Sr _{1.2} Bi _{2.4} Ta _{2.0} O ₉ and Bi
Substrate	RuO ₂ /Si
Base pressure of system	1.2 × 10 ⁻⁵ torr
Sputtering pressure	10 mtorr
r.f sputtering power	100 W
Sputtering gas (Ar : O ₂)	1 : 1
Substrate temperature	500°C

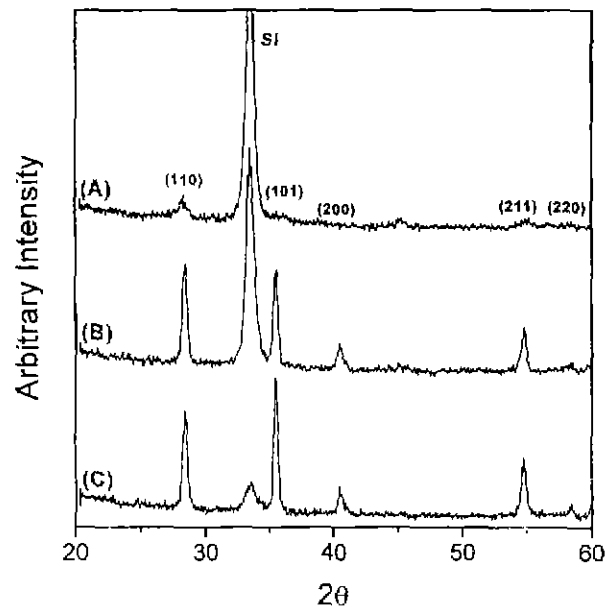
get to control the Bi content in SBT films. The SBT films deposited at 500°C were annealed at 800°C for 30 min in oxygen ambient. The detailed sputtering conditions of SBT thin films are summarized in Table 2.

The crystal structure of the films was characterized by X-ray diffraction (XRD) employing Cu K α radiation and a Ni filter. The microstructure of the films was investigated with transmission electron microscopy (TEM). The morphology and the thickness of the films were determined with a scanning electron microscope (SEM). The film composition was determined by electron probe X-ray microanalysis (EPMA) and the resistivity of RuO₂ films was measured with a four-point probe.

For electrical measurements, top electrodes of platinum (80 nm thickness and 100 μ m diameter) were deposited by dc sputtering using a shadow mask to prepare Pt/SBT/RuO₂/Si capacitors. Ferroelectric properties were measured using a RT 66A ferroelectric tester (Radiant technology) operating in virtual ground mode. The current-voltage (I-V) measurements were performed with a Keithley 617 programmable electrometer. The leakage current behavior was determined with a voltage step of 0.1 V and delay time of 1 sec.

III. Results and Discussion

Figure 1 shows the X-ray diffraction (XRD) patterns of the RuO₂ thin films deposited on Si substrate at various deposition temperatures. The XRD patterns of films deposited at 220°C (Fig. 1(A)) shows only broad (110) peak, which indicates that the film is not completely crystallized. But the XRD patterns at 250°C (Fig. 1(B)) show the peaks indicating the (110), (101), (200) and (211) planes. RuO₂ single phase was obtained at such a low

**Fig. 1.** X-ray diffraction (XRD) patterns of the RuO₂ thin films deposited on Si substrate at the deposition temperatures: (A) 220, (B) 250 and (C) 270°C.

temperature of 250°C. The deposition of RuO₂ at low temperature is possible because the mixtures of ruthenocene (Ru(C₅H₅)₂) and oxygen were already activated before reaching at the substrate surface to form a RuO₂ phase in hot-wall system. The crystallinity of RuO₂ thin films improved with increasing deposition temperature, films show the random orientation at all deposition temperatures.

Figure 2 shows the plan-view SEM images of the RuO₂ thin films deposited at various temperatures. In Fig. 2(A), the RuO₂ thin film deposited at 220°C shows the fine grains, which indicate that the films are not completely crystallized. In Fig. 2(B) and (C), the grain size of RuO₂ films drastically increases with increasing deposition temperature.

Figure 3 shows cross-sectional and plan-view TEM images for RuO₂ thin films deposited at 270°C. The average grain size is about 45 nm, as shown in Fig. 3(A). The holes observed along some grain boundaries and grain boundary triple points are artifacts of the sample preparation for TEM analysis. The sample was thinned from the back side by ion milling. At the surface of the RuO₂ film, which has a certain roughness, the ion milling caused the formation of the holes at grain boundaries. RuO₂ thin films grow perpendicularly to the substrate and show the columnar structure, as shown in Fig. 3(B). A close inspection reveals a somewhat conical shape of the columns, with the tips of the cones pointing towards the substrate.

Figure 4 shows the high resolution TEM micrograph with an imaging magnification of 2.0 × 10⁸ of RuO₂ thin films deposited at 270°C. The interlayer observed between the RuO₂ film and Si substrate is SiO₂. At the

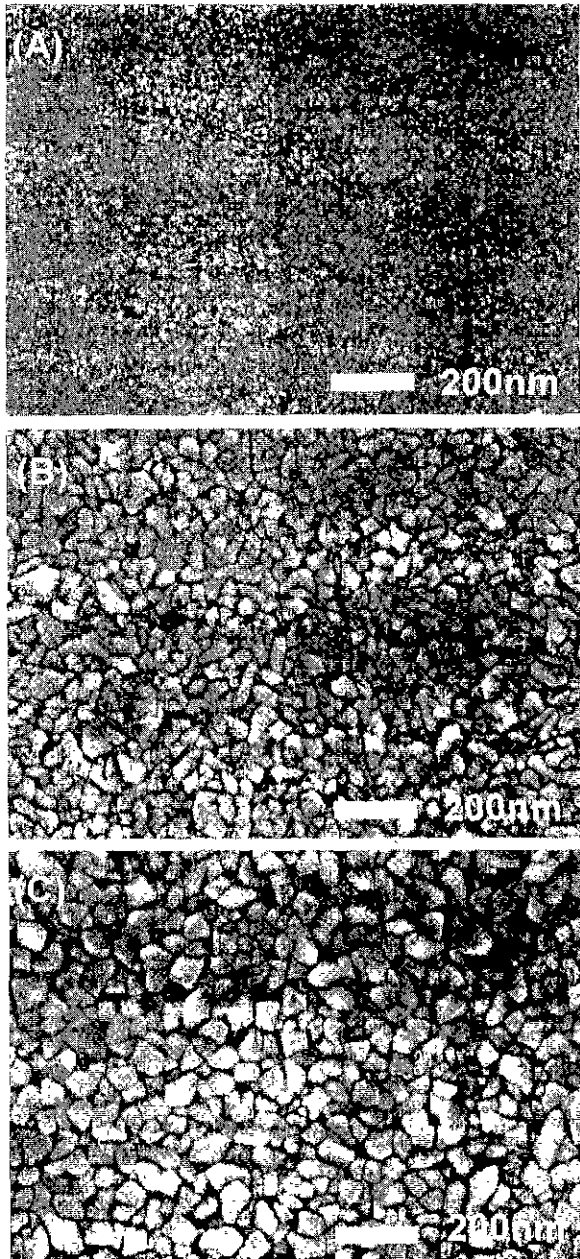


Fig. 2. SEM surface images of RuO₂ thin films deposited on Si for various deposition temperatures ((A) 220, (B) 250 and (C) 270°C).

initial stage of deposition, Si substrate was exposed in oxygen ambient, and then the SiO_x interlayer was formed. The thickness of SiO_x interlayer is about 35 Å. By energy dispersive X-ray spectroscopy(EDS) analysis, the interdiffusion between the RuO₂ and Si was not observed and the Ru-silicide was not formed at interface.

Figure 5 shows the variation of film resistivity vs. thickness of RuO₂ films deposited at 270°C. The resistivity of the 180 nm-thick RuO₂ thin films was 136 μΩ-cm and the resistivity increased with decreasing film thickness. The inset of Fig. 5 shows the relationship between the average grain size and the film thickness.

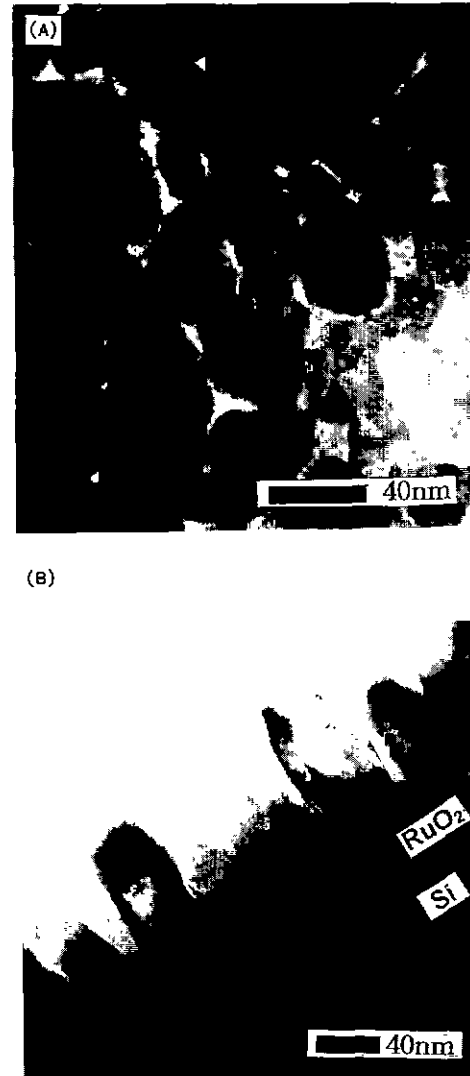


Fig. 3. (A) plan-view and (B) Cross-sectional TEM images of RuO₂ thin films deposited at 270°C.

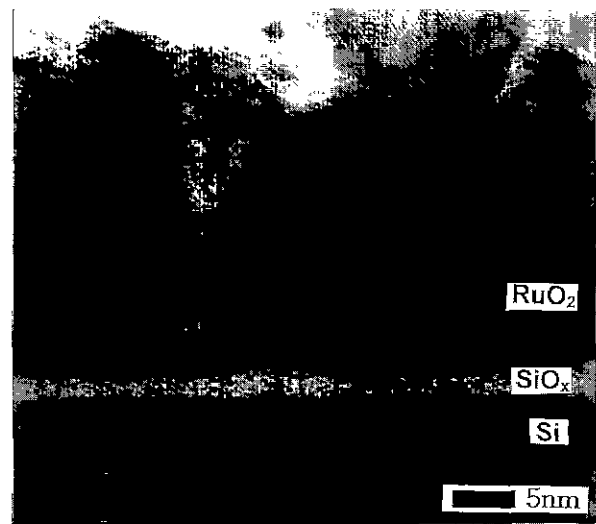


Fig. 4. High resolution TEM micrograph of RuO₂ thin films deposited on Si at 270°C.

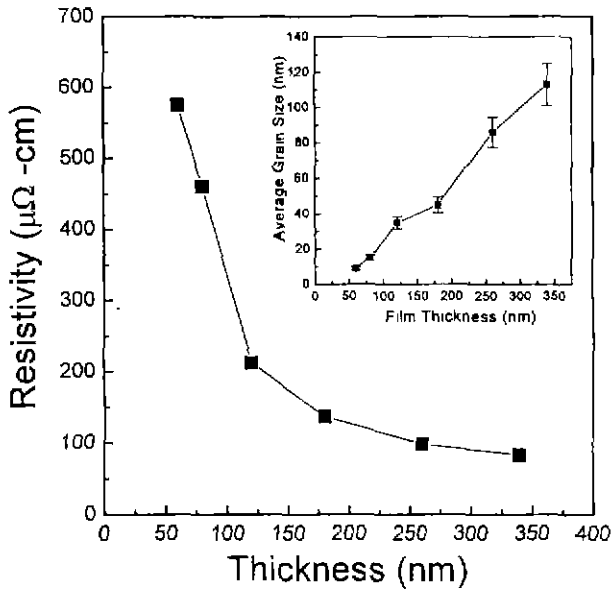


Fig. 5. The resistivity of RuO₂ thin films deposited at 270°C as a function of film thickness

The average grain size increased linearly with increasing film thickness. The surface of the films thinner than 100 nm consisted of fine grains from the TEM observation. These results consist with the prediction of the grain boundary scattering theory of Mayadas and Shatzkes(MS),¹²⁾ in which the mobility is decided by the grain boundaries while the carrier concentration is taken to be a constant.

Figures 6 (A) and (B) show the X-ray diffraction patterns of SrBi₂Ta₂O₉ thin films and target, respectively. Thin films were deposited on RuO₂/Si at 500°C and then

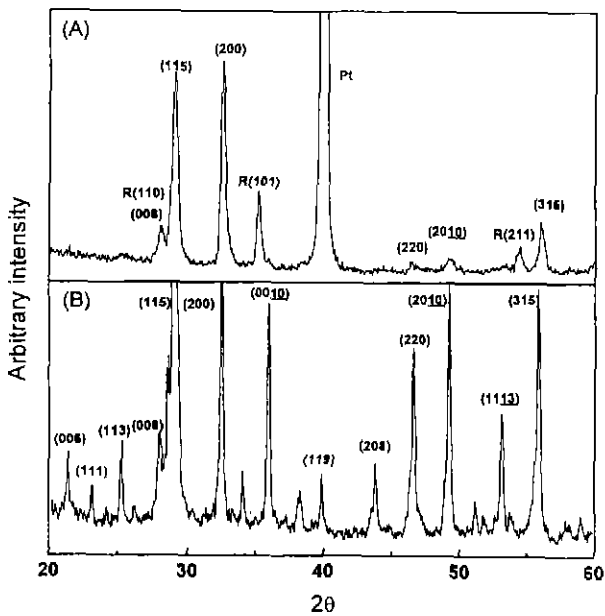


Fig. 6. X-ray diffraction patterns of (A) SrBi₂Ta₂O₉ thin film annealed at 800°C for 30 min in oxygen ambient after depositing on RuO₂/Si at 500°C and (B) SBT target.

annealed at 800°C for 30 min in oxygen ambient. The target shows the peaks of the orthorhombic structure, which coincide with Riedveld simulation pattern using lattice parameters calculated by Rae *et al.*¹³⁾ Any second phase did not exist in the target. Therefore, the used target was suitable for preparation of films by rf magnetron sputtering. The films annealed at 800°C for 30 min have a strong intensities of (115) and (200) peaks. These results suggested that SBT films indicated very well crystallized films and showed a randomly oriented orthorhombic structure. The Pt peak at the films deposited on RuO₂/Si was due to the Pt top electrode.

Figure 7 shows the typical SEM images of SBT films annealed at 800°C for 30 min in oxygen ambient after depositing on RuO₂/Si at 500°C. The RuO₂ bottom electrode is stable after annealing at 800°C. The SBT films de-

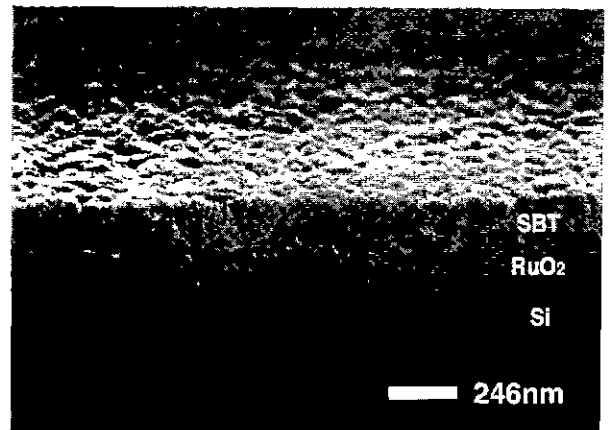


Fig. 7. SEM image of SBT thin film annealed at 800°C for 30 min in oxygen ambient.

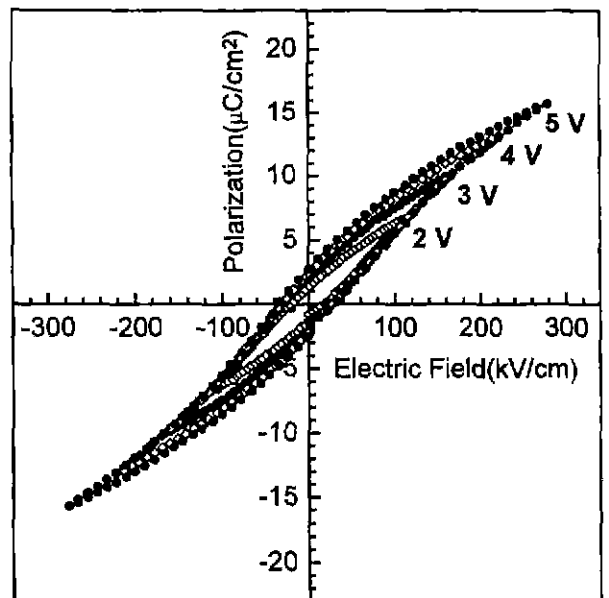


Fig. 8. The hysteresis loop of SBT/RuO₂/Si film annealed at 800°C.

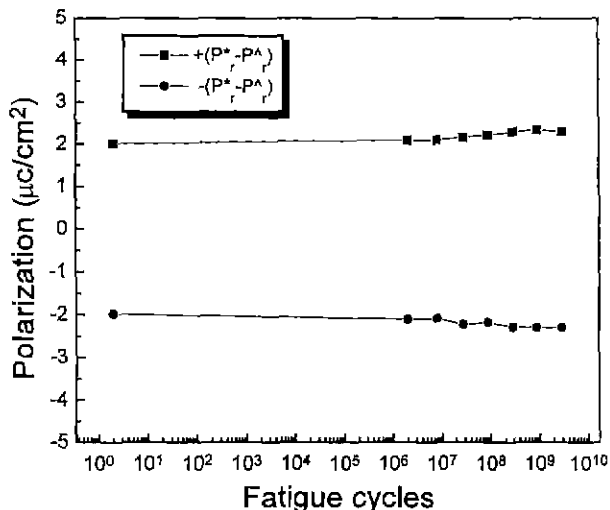


Fig. 9. Fatigue characteristics of SBT thin films deposited on RuO₂/Si.

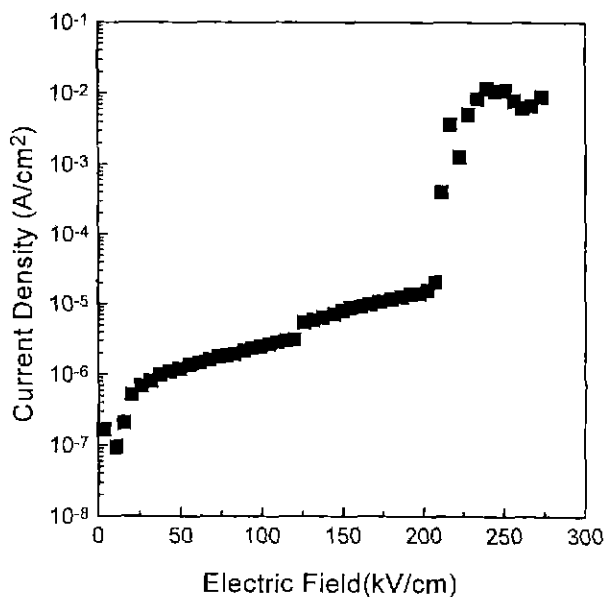


Fig. 10. The leakage current characteristics of SBT/RuO₂/Si film annealed at 800°C.

posited on RuO₂/Si have a dense and smooth microstructure.

The hysteresis loop of Pt/SBT/RuO₂/Si is shown in Fig. 8. The SBT/RuO₂/Si film was annealed at 800°C for 30 min in oxygen ambient. The loops were saturated at 3 V and showed low coercive field. The remanent polarization, 2 P_r, and the coercive field, 2 E_c, of SBT thin films deposited on RuO₂/Si were about 5.2 µC/cm² and 76.0 kV/cm at an applied voltage of 5 V, respectively. Although the polarization value is small, the coercive field is less than that reported by Desu *et al.*¹⁴ The low coercive field is attractive for the ferroelectric random access memory (FRAM) application.

Figure 9 shows the fatigue characteristics of 190 nm-thick SBT thin films deposited on the RuO₂/Si. Fatigue

test was done using a 5 V bipolar square pulse at 1 MHz introduced by function generator. As shown in Fig. 9, SBT films show practically no polarization fatigue up to ~10¹⁰ cycles. Furthermore, the shape of the hysteresis loop does not change with switching cycles.

Figure 10 shows the leakage current characteristics of SBT/RuO₂/Si film annealed at 800°C. The leakage current by positive bias was measured with a voltage step of 0.1 V and delay time of 1 s. The leakage current density of the 190-nm thick SBT film was 7.0 × 10⁻⁶ A/cm² at 150 kV/cm.

IV. Conclusions

RuO₂ thin films were prepared on Si(100) by hot-wall metalorganic chemical vapor deposition using the ruthenocene and oxygen gas mixtures. RuO₂ single phase was obtained at low deposition temperature of 250°C. The average grain size of RuO₂ thin film deposited at 270°C is about 45 nm. The resistivity of the 180 nm-thick RuO₂ thin films deposited on Si at 270°C was 136 µΩ-cm and the resistivity increased with decreasing film thickness.

The remanent polarization, 2 P_r, and the coercive field, 2 E_c, obtained for a 190 nm-thick SBT films deposited on RuO₂/Si were 5.2 µC/cm² and 76.0 kV/cm for an applied voltage of 5V, respectively. The films showed a fatigue-free characteristics up to ~10¹⁰ cycles under 5 V bipolar square pulses. The leakage current density of SBT thin film was about 7.0 × 10⁻⁶ A/cm² at 150 kV/cm. RuO₂ thin films are concluded to be promising electrodes for non-volatile random access memory (NVRAM) device application.

Acknowledgements

The authors would like to thank Mr. Jong-Bong Park and Dr. Joong-Whan Lee of Korea Material Analysis Corp. for Transmission electron Microscope observations.

References

1. J. F. Scott and C. A. Paz de Araujo, *Science* **246**, 1400 (1989).
2. S. K. Dey and Zuleeg, *Ferroelectrics* **108**, 37 (1990).
3. H. N. Al-shareef, B. A. Tuttle, W. L. Warren, T. J. Headley, D. Dimos, J. A. Voigt and R. D. Nasby, *J. Appl. Phys.* **79**, 1013 (1996).
4. M. L. Green, M. E. Gross, L. E. Papa, K. J. Schnoes and D. Brasen, *J. Electrochem. Soc.* **132**, 2677 (1985).
5. L. Krusin-Elbaum, M. Wittmer and D. S. Yee, *Appl. Phys. Lett.* **50**, 1979 (1987).
6. Q. X. Jia, L. H. Chang and W. A. Anderson, *J. Mater. Res.* **9**, 2561 (1994).
7. H. N. Al-Shareef, K. R. Bellur, A. I. Kingon and O. Auciello, *Appl. Phys. Lett.* **66**, 239 (1995).
8. S. Y. Mar, J. S. Liang, C. Y. Sun and Y. S. Huang, *Thin Solid Films* **238**, 158 (1994).

9. J. Si and S. B. Desu, *J. Mater. Res.* **8**, 2644 (1993).
10. E. Kolawa, F. C. T. So, W. Flick, X. A. Shao, E. T.-S. Pan and M. A. Nicolet, *Thin Solid Films* **173**, 217 (1989).
11. T. S. Kalkur and Y. C. Lu, *Thin Solid Films* **205**, 266 (1991).
12. A. F. Mayadas and M. Shatzkes, *Phys Rev. B*, **1**, 1382 (1970).
13. A. D. Rae, J. G. Thompson and R. L. Withers, *Acta Cryst. B* **48**, 418 (1992).
14. S. B. Desu and D. P. Vijay, *Mater. Sci. Eng. B* **32**, 83 (1995).